

AD\_\_\_\_\_

Award Number: DAMD17-97-1-7053

TITLE: Response of Breast Cancer Cells to Hormonal Therapy;  
Quantitative in Vivo NMR Studies

PRINCIPAL INVESTIGATOR: Douglas S. Clark, Ph.D.

CONTRACTING ORGANIZATION: University of California

Berkeley, California 94720

REPORT DATE: September 1999

TYPE OF REPORT: Annual

PREPARED FOR: U.S. Army Medical Research and Materiel Command  
Fort Detrick, Maryland 21702-5012

DISTRIBUTION STATEMENT: Approved for public release;  
distribution unlimited

The views, opinions and/or findings contained in this report are those of the author(s) and should not be construed as an official Department of the Army position, policy or decision unless so designated by other documentation.

20010216 110

# REPORT DOCUMENTATION PAGE

*Form Approved  
OMB No. 074-0188*

Public reporting burden for this collection of information is estimated to average 1 hour per response, including the time for reviewing instructions, searching existing data sources, gathering and maintaining the data needed, and completing and reviewing this collection of information. Send comments regarding this burden estimate or any other aspect of this collection of information, including suggestions for reducing this burden to Washington Headquarters Services, Directorate for Information Operations and Reports, 1215 Jefferson Davis Highway, Suite 1204, Arlington, VA 22202-4302, and to the Office of Management and Budget, Paperwork Reduction Project (0704-0188), Washington, DC 20503

<b>1. AGENCY USE ONLY (Leave blank)</b>			<b>2. REPORT DATE</b> September 1999		<b>3. REPORT TYPE AND DATES COVERED</b> Annual (15 Aug 98 - 14 Aug 99)	
<b>4. TITLE AND SUBTITLE</b> Response of Breast Cancer Cells to Hormonal Therapy; Quantitative in Vivo NMR Studies			<b>5. FUNDING NUMBERS</b> DAMD17-97-1-7053			
<b>6. AUTHOR(S)</b> Douglas S. Clark, Ph.D.						
<b>7. PERFORMING ORGANIZATION NAME(S) AND ADDRESS(ES)</b> University of California Berkeley, California 94720			<b>8. PERFORMING ORGANIZATION REPORT NUMBER</b>			
<b>E-MAIL:</b> clark@cchem.berkeley.edu						
<b>9. SPONSORING / MONITORING AGENCY NAME(S) AND ADDRESS(ES)</b> U.S. Army Medical Research and Materiel Command Fort Detrick, Maryland 21702-5012			<b>10. SPONSORING / MONITORING AGENCY REPORT NUMBER</b>			
<b>11. SUPPLEMENTARY NOTES</b>  This report contains colored photos						
<b>12a. DISTRIBUTION / AVAILABILITY STATEMENT</b> Approved for public release; distribution unlimited						<b>12b. DISTRIBUTION CODE</b>
<b>13. ABSTRACT (Maximum 200 Words)</b>  <p>Our research is directed at determining the specific metabolic pathways and the individual reactions affected by estrogen and tamoxifen in both estrogen receptor-positive (ER+) and estrogen receptor-negative (ER-) breast cancer cells through the use of novel NMR methodology and quantitative analysis. In this report period, we have quantified the effect of estrogen on metabolic fluxes in ER+ cells. This was accomplished using a comprehensive metabolic model and NMR data from cell extracts. The model was further refined to allow for the incorporation of isotopomer, or multiply-labeled, metabolite data. Microcarrier culture, flask, and roller bottle studies were continued in order to expand the methodology used to quantify breast cancer cell metabolism under varied treatment conditions. In addition, investigations were performed in flasks to characterize the dose response of cells to the metabolic inhibitor cerulenin.</p>						
<b>14. SUBJECT TERMS</b> Breast Cancer						<b>15. NUMBER OF PAGES</b> 22
						<b>16. PRICE CODE</b>
<b>17. SECURITY CLASSIFICATION OF REPORT</b> Unclassified	<b>18. SECURITY CLASSIFICATION OF THIS PAGE</b> Unclassified	<b>19. SECURITY CLASSIFICATION OF ABSTRACT</b> Unclassified	<b>20. LIMITATION OF ABSTRACT</b> Unlimited			

## **TABLE OF CONTENTS**

Standard Form 298.....	p.2
Foreword.....	p.4
Introduction.....	pp.5-6
Body.....	pp.6-14
Key Research Accomplishments.....	p.14
Reportable Outcomes.....	pp.14-15
Conclusions.....	p.15
Figures.....	pp.16-21
References.....	p.22

FOREWORD

Opinions, interpretations, conclusions and recommendations are those of the author and are not necessarily endorsed by the U.S. Army.

       Where copyrighted material is quoted, permission has been obtained to use such material.

       Where material from documents designated for limited distribution is quoted, permission has been obtained to use the material.

       Citations of commercial organizations and trade names in this report do not constitute an official Department of Army endorsement or approval of the products or services of these organizations.

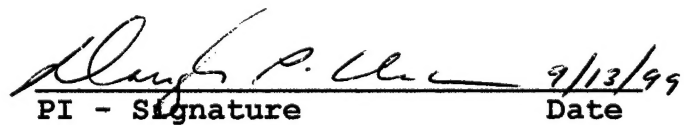
N/A In conducting research using animals, the investigator(s) adhered to the "Guide for the Care and Use of Laboratory Animals," prepared by the Committee on Care and use of Laboratory Animals of the Institute of Laboratory Resources, national Research Council (NIH Publication No. 86-23, Revised 1985).

X For the protection of human subjects, the investigator(s) adhered to policies of applicable Federal Law 45 CFR 46.

N/A In conducting research utilizing recombinant DNA technology, the investigator(s) adhered to current guidelines promulgated by the National Institutes of Health.

N/A In the conduct of research utilizing recombinant DNA, the investigator(s) adhered to the NIH Guidelines for Research Involving Recombinant DNA Molecules.

N/A In the conduct of research involving hazardous organisms, the investigator(s) adhered to the CDC-NIH Guide for Biosafety in Microbiological and Biomedical Laboratories.

  
Dray P. Clark  
PI - Signature      Date  
9/13/95

## **INTRODUCTION**

Breast cancer, the most prevalent cancer among women, has proven to be a devastating disease. The pain of being diagnosed with the disease is compounded by the lack of a definitive treatment. Currently, the most widely used post-operative hormonal therapeutic is the antiestrogen tamoxifen (TAM). TAM acts at least in part as a competitive inhibitor of estrogen, a hormone which signals cell growth in breast cells. Although effective in postmenopausal patients with estrogen receptor-positive (ER+) tumors, its effectiveness in premenopausal patients and in patients with estrogen receptor-negative (ER-) tumors is substantially lower. Additionally, TAM resistance and cancer recurrence strikes almost all patients with advanced breast cancer undergoing TAM therapy<sup>1</sup>. The serious limitations of this current treatment highlight the need for a greater understanding of both estrogen and TAM action.

A consequence of anti-cancer therapy is an alteration of carbon flows through metabolic pathways. Changes in metabolic fluxes allow cells to provide cellular components to accommodate increased growth. In human breast cancer cells, increased growth and consequent metabolic changes are initiated by estrogen binding to the estrogen receptor. Conversely, TAM is a cytostatic drug which appears to compete with endogenous estrogen for binding to the ER, preventing communication of the growth signal. The effect of this broken communication on metabolism is presently not known. The proposed research uses novel methodology to identify the specific metabolic pathways and the individual metabolic reactions affected by estrogen and TAM in both ER+ and ER- cells. The metabolic effects of these agents, manifested as changes in metabolic fluxes, will be quantified with the aid of NMR techniques. This will enable a description of the relationship between primary metabolism and growth of cells in response to estrogen and TAM treatment to be developed. This new information will help guide the development of new therapies and new therapeutic agents for arresting the metabolism of breast cancer cells and tumors. The specific purposes stated in the original proposal were as follows:

- *Identify the primary metabolic pathways that are operative in ER+ and ER- cells.* This will be achieved by *in vivo* <sup>13</sup>C NMR tracer studies and extracellular measurements of ER+ and ER- cells grown in a hollow fiber bioreactor (HFBR).
- *Quantify the primary and secondary metabolic fluxes in breast cancer cells in the presence and absence of TAM and estrogen, including those effects which may be reversed by increased concentrations of estrogen ("estrogen rescue"), and those effects of TAM that are not related to ER binding.* Flux and label balance equations will be developed for carbon pathways. Using both extracellular assays and *in vivo* NMR measurements of cells grown in an HFBR, these equations will be solved to determine metabolic fluxes in response to estrogen and TAM treatment. Fluxes through branchpoints, indeterminable by extracellular measurements alone, can be quantified using this methodology.
- *Examine modes of estrogen and tamoxifen action by investigating the relationship between fatty acid synthesis and the pentose phosphate pathway, and other pathways requiring NADP<sup>+</sup>/NADPH.* We will examine the effects of impaired fatty acid synthesis (resulting from the addition of the fatty acid synthase inhibitor, cerulenin) on other metabolic pathways in the presence of estrogen and tamoxifen.

In this report period, we have made significant progress toward all three goals. Additional experiments to determine the metabolic requirements of ER+ MCF7 cells have been performed in microcarrier culture. Microcarrier culture, flask, and roller bottle studies were performed in order to develop and demonstrate the ability to quantify breast cancer cell metabolism under varied treatment conditions. Metabolic fluxes were calculated for estrogen-rescued cells using NMR data from cell extracts and our metabolic model. We have determined that flux analysis using cell extract NMR data is significantly more accurate than that using *in vivo* data; thus all flux determinations were based on cell extract data.

## **BODY**

### **A. Methods and Procedures**

#### **1. General Methods**

*Cell Cultures.* Human breast cancer cell lines T47D and MCF7 were obtained from American Type Culture Collection and maintained in Dulbecco's Modified Eagle's Medium (DMEM) with 5% fetal bovine serum (FBS) at 37°C in a humidified atmosphere with 5% CO<sub>2</sub>. Confluent Falcon tissue culture flasks were subcultured weekly following trypsinization with 0.05% trypsin in saline /ethylaminodiaminetetraacetic acid (EDTA). Cell counts were obtained using a Coulter Multisizer or Neubauer hemacytometer.

*Glucose, Lactate, and Amino Acid Measurements.* Glucose and lactate concentrations were determined using a Yellow Springs Instrument Co. 2700 Select Biochemistry Analyzer. Amino acid concentrations were determined using an Applied Biosystems 130A high pressure liquid chromatography system (HPLC) and 420A derivatizer equipped with a 920 data module.

*Roller Bottle Culture.* Cells were grown in 850 cm<sup>2</sup> Falcon or Corning roller bottles. After seeding at 15,000 - 20,000 cells/cm<sup>2</sup>, the bottles were rotated at 1/3 RPM for twenty-four hours and at 1 RPM thereafter<sup>2</sup>. The headspace of the bottles was purged with 5% CO<sub>2</sub> in air.

#### **2. TAM Effects in MCF7 Microcarrier Cultures**

Cells were seeded in spinner flasks containing 0.67 g/L Cytodex 3 microcarriers (Pharmacia) and 50,000-60,000 cells/ml (15,625-18,750 cells/cm<sup>2</sup>). Cultures were initiated in 2/5 of the final culture volume and stirred for 2 minutes every half hour for the first five hours. After this time, cultures were brought up to a final volume of 500 ml and stirred constantly at 60 RPM. Culture media was replaced with TAM or vehicle control-containing media 24 hours after initiation (day 0). Samples were removed daily for determination of cell number. Three samples were removed for each time point. Released nuclei stained with crystal violet were counted on a hemacytometer<sup>4</sup>. Media samples were also removed regularly for glucose, lactate and amino acid measurement. Cell pellets were prepared for cell cycle analysis using flow cytometry. Flow cytometry measurements of propidium iodide-stained nuclei were obtained using a Coulter EPICS-XL flow cytometer.

#### **3. Cell Extraction**

Cells were removed from either bottles or flasks by trypsinization and then pelleted by centrifugation at 1200 RPM for 5 minutes. Cell pellets were treated with 1 ml 5% perchloric acid (PCA) per 250 µl of cell volume. Cell solids were removed by centrifugation and the supernatent neutralized with 250 µl of 2M K<sub>2</sub>CO<sub>3</sub>. Precipitated potassium perchlorate was removed and the extract

dried by lyophilization<sup>5</sup>. Extracts were stored at -4°C and rehydrated in 250 µl of D<sub>2</sub>O just prior to NMR analysis.

Using extraction to characterize the intracellular isotope distribution and subsequently determine intracellular fluxes has been questioned because of concerns that extraction affects the chemical make-up of the isotope-containing metabolites. However, preliminary measurements indicated that the major metabolites observable in breast cancer cells by <sup>13</sup>C-NMR are the amino acids glutamate and aspartate, both of which are unaffected by acid extraction.

There are many advantages to the extraction NMR method when compared to the proposed *in vivo* methods. High concentrations of intracellular aspartate and glutamate can be attained that produce very informative spectra on a high powered 500 MHz spectrometer. In these spectra, isotopomers, or multiply labeled species, can be discerned. A measured isotopomer distribution can be used to increase the accuracy of the calculated fluxes. In addition, numerous flasks or bottles can be grown simultaneously prior to extraction. Investigating different treatments and controls concurrently allows efficient comparison of treatments and verification of their metabolic consequences.

#### **4. Metabolic Response to Estrogen Rescue Treatment Using 1-<sup>13</sup>C NMR and Cell Extraction**

Six roller bottles were seeded with MCF7 cells. Samples of the bulk media were taken every 8 hours to determine the concentrations of glucose, lactate, and the amino acids. The experiment lasted for 8 days. The bottles were fed medium containing 5 µM tamoxifen on the first and third days. On the fifth day media containing 1-<sup>13</sup>C glucose was supplied to all six bottles. Three bottles also received 0.5 µM estrogen. This cell cycle hold-up followed by stimulation is the basis of estrogen rescue. On the seventh day the cytoplasm of all the cells in each of the six bottles was extracted. All six bottles were trypsinized and the cell pellet resuspended in 8 ml of conditioned medium. Conditioned medium was used to limit transport of unlabeled metabolites into the cells. A small portion of this resuspension (0.2 ml) was used for cell density determination on a Coulter Counter. The remainder of the cells were re-centrifuged and used for extraction.

#### **5. NMR Analysis**

<sup>13</sup>C spectra were acquired on a 500MHz Bruker DRX spectrometer with a 5 mm broad-band probe. A ninety-degree pulse was used with a 6 second interscan delay. Spectra were acquired overnight, resulting in the signal averaging of approximately 5600 scans. Concentrations of labeled species were determined by calibration to a 2 mM ethylene glycol peak.

#### **6. Development of a Biochemical Pathway Model and Mathematical Description**

Measured external metabolite fluxes and fractional enrichments were inputted into a mathematical description of biochemical pathways to determine the unknown internal fluxes. In batch growth (flask and roller bottle culture), external fluxes,  $f_{i,ex}$  (µmol/cell·hr), are calculated from linear time-course concentration profiles using equation 1<sup>6</sup>:

$$f_{i,ex} = \frac{1}{N} \cdot \frac{dC_i}{dt} = \frac{b_i}{N} \quad (1)$$

where  $C_i$  is the concentration of metabolite  $i$ ,  $N$  is number of cells and  $b_i$  is the slope of the linear concentration profile. Currently the metabolically important substrates that are measured are glucose, lactate, glutamate, glutamine, aspartate, serine, and alanine. Fractional enrichments are determined by

integrating decoupled carbon spectra to determine the concentration of label,  $L_{i,y}$ , on atom y in metabolite i. The total metabolite concentration in the extract,  $C_i$ , was measured by HPLC or enzyme assay and was combined with the concentration of label to calculate the absolute fractional enrichment,  $M_{i,y}$ :

$$M_{i,y} = \frac{L_{i,y}}{C_i} \quad (2)$$

Conversion of fractional enrichments and external flux data into internal fluxes requires the development of a biochemical pathway model. It is impossible to include all of the many pathways in a single model. Pathways retained in the model have either significant flows of carbon or considerable effects on the isotope distribution. The current model is shown in Figure 1 (see next page) and contains the following pathways: glycolysis, the TCA cycle, the pentose phosphate pathway, glutaminolysis, malate transport, tricarboxylate transport, malic enzyme, and pyruvate carboxylase.

Fluxes are calculated using metabolite and isotope mass balances. Because metabolic steady state is assumed<sup>7</sup>, the intracellular accumulation is negligible, and metabolite balances simply equate the sum of the fluxes producing a metabolite to the sum of the fluxes consuming it. All of the balances derived from Figure 1 are given in Table 1:

**Table 1 Metabolite balances derived from Figure 1**

$f_1 = f_2 + f_3$ $f_2 + 2/3 f_3 = f_4$ $f_4 = 2 f_5$ $f_5 + 1/3 f_3 = f_6$ $f_6 + f_7 + f_{20} = f_{10} + f_{11} + f_{12} + f_{19}$	$f_{12} + f_{24} = f_{14}$ $f_{14} = f_{13} + f_{16}$ $f_{15} + f_{16} + f_{22} = f_{17} + f_{18} + f_{21} + f_{25}$ $f_{17} + f_{18} + f_{19} = f_9 + f_{14}$ $f_9 + f_{13} = f_{20}$
--	--

Isotope balances equate the sum of the fluxes of isotope into a single *atom* of a metabolite to the sum of the fluxes out.

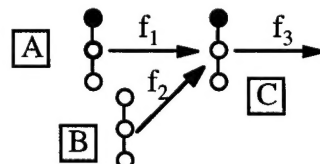


**Figure 2. Example of an isotope balance.** Each circle represents carbon atoms in one of three example molecules: A, B and C. The darkened circles are partially enriched by  $^{13}\text{C}$ . The three carbon atoms of each molecule are numbered 1 - 3 starting at the top. This particular set of reactions represents the recombination of two pathways.

The isotope balance around the first carbon of metabolite C in Figure 2 is written as

$$f_1 \cdot A1 + f_2 \cdot B1 = f_3 \cdot C1 \quad (3)$$

Where A1, B1, and C1 are the fractional enrichments of the first carbons of metabolite A, B, and C, respectively. The product of  $f_i \cdot C$  thus has units of  $\mu\text{mol}/\text{cell} \cdot \text{hr}$ . Two more balances can be written for the example, one for the second carbon and one for the third. An isotope balance in this form can be written around every atom of every metabolite in the pathway model. In Figure 1 there are 44 such balances. Because very few of the enrichment fractions were actually measured, it was necessary to

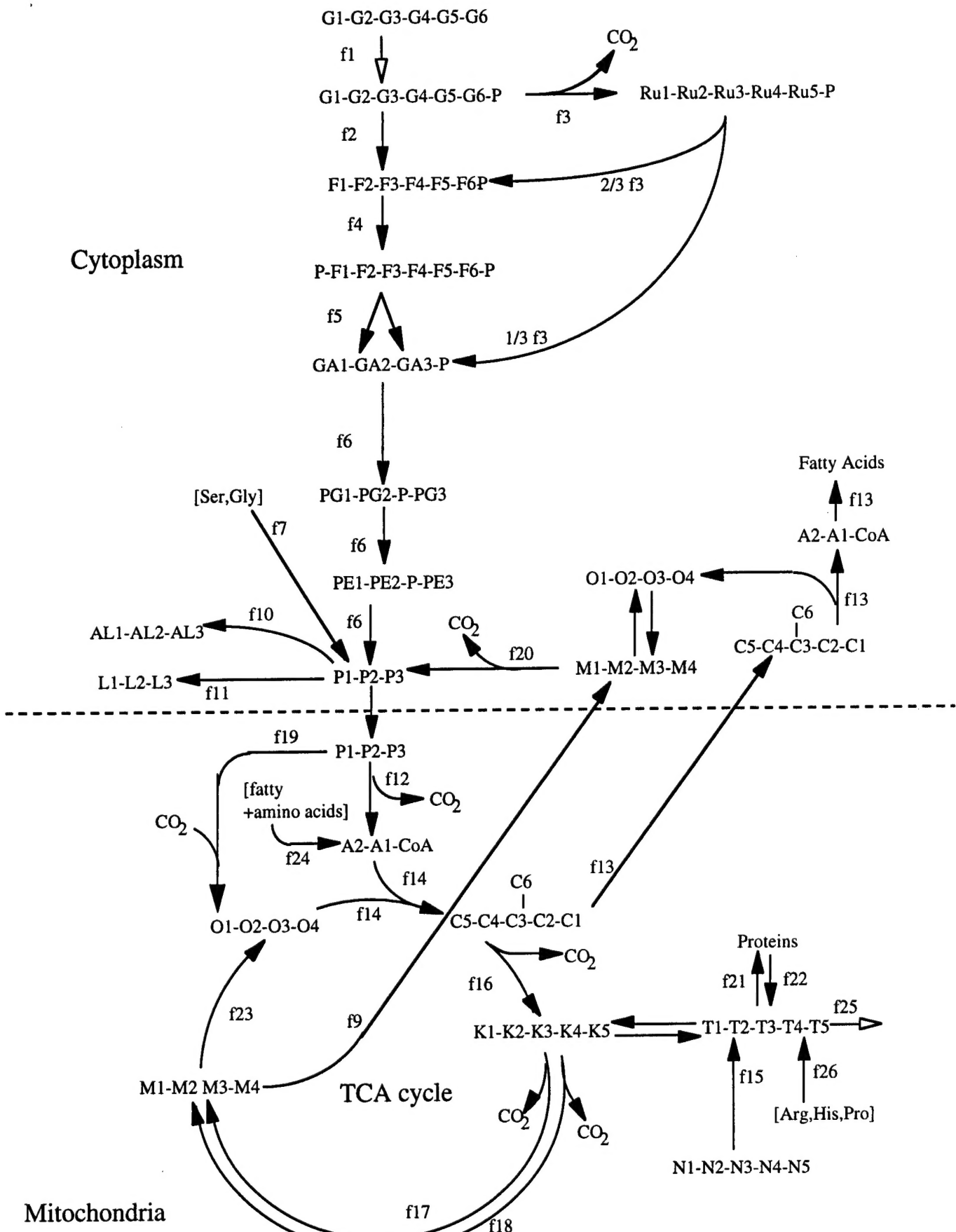


Figure 1. Current metabolic pathway model. Abbreviations are: G-glucose, Ru-ribose-5-phosphate, F-fructose, GA-glyceraldehyde-3-phosphate, PG-phosphoglycerate, PE-phophenolpyruvate, P-pyruvate, AL-alanine, L-lactate, M-malate, O-oxaloacetate, C-citrate, A-acetyl-CoA, K-a-ketoglutarate, T-glutamate, and N-glutamine.

reduce the number of equations. It was possible to produce 5 equations for each of the five isotope measurements made.

The method of least squares was used to find the set of unknown fluxes by minimization of the sum-of-squares, F, which is given by

$$F = \sum_{i=1}^n \frac{[y_i - y_i(x)]^2}{\sigma_i^2} \quad (14)$$

where  $y_i$  is any measured value, either fractional enrichment or external flux, and  $y_i(x)$  is the adjusted value of that variable constrained by the metabolite and isotope balances. There are n measurements and x represents the adjusted unknown fluxes. The standard deviation of each measurement,  $\sigma_i$ , is included to weigh the sum in favor of more accurate measurements.

Errors in the values of the internal fluxes were calculated by simulation around the errors of the input measurements<sup>8</sup>. This is done by first generating a statistically probable set of input data inside a Gaussian distribution of the measurements. A new set of internal fluxes was calculated from this new set of input "data." This process is repeated M times, after which the error of each internal flux is given by

$$E_i = \sqrt{\sum_{j=1}^M (f_{ij} - \hat{f}_i)^2 / M} \quad (15)$$

where  $\hat{f}$  is the set of best-fit fluxes, determined from the initial values of the measurements. These errors of the internal fluxes have three purposes: they establish the accuracy of the results, they discriminate plausible from implausible pathway models, and they establish the statistical significance between different test conditions.

## 7. Isotopomers and Simulated Annealing

Advances in experimental techniques enabled the detection of isotopomers in internal metabolites by NMR as shown in Figure 3. That the concentration of these multiply labeled metabolites can be used in the analysis to increase the accuracy of flux results and add more pathways to the biochemistry model is a significant finding of our research. The only pathway that joins together metabolites in Figure 1, and hence is able to form isotopomers, is the citrate synthase pathway. Because citrate synthase is contained within the mitochondria and isotopomers accumulate in extra-mitochondrial pools, additional pathways in and out of the mitochondria were added.

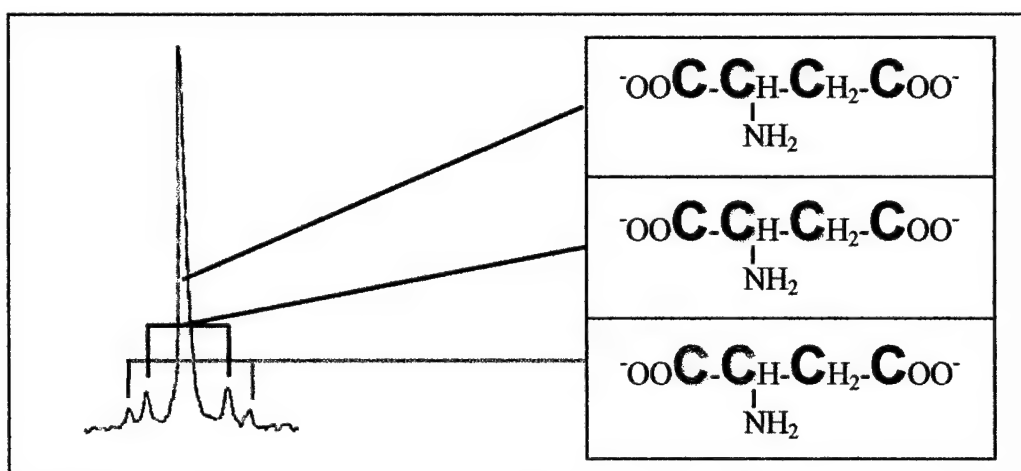


Figure 3. Isotopomers of aspartate visible in a <sup>13</sup>C-NMR spectrum of an MCF7 cell extraction by perchloric acid following estrogen stimulation

In order to use isotopomer measurements to calculate fluxes, the analysis method had to be enhanced. The problem encountered was that the desired results, determining all of the fluxes in Figure 1, could not be calculated from the available data, a set of extra-cellular fluxes and a set of internal metabolite isotopomer concentrations. There were two major limitations in achieving this goal. The first is the scope of the problem, i.e. the large number of variables and equations. Any method for determining a set of fluxes is based on isotopomer balances, which are similar in form to the isotope balances in equation 3. However, if a balance for every isotopomer of each metabolite was considered (there are over 1000), the problem would be intractable. The second restriction was that it was not possible to recast the isotopomer balances into a simple analytical form that would express each flux as a function of the isotopomer measurements alone:

$$\text{flux}_i = f(\text{all isotopomers}) \quad (4)$$

This is due to the non-linear relation between isotopomer measurement and flux, and the self-dependent nature of cyclic biological pathways. Therefore, a numerical approach based on a simulated annealing algorithm was used to address these issues.

The premise of the simulated annealing algorithm involved guessing an initial set of fluxes and calculating the accompanying isotopomer pattern. These calculated isotopomers were compared to the measured values and then a new set of fluxes was guessed. This cycle was repeated until the difference between the guessed and measured isotopomer concentrations reached a minimum. This method allows a global minimum to be approached in a highly-dimensional non-linear system.

The intractability of the system was encountered when the isotopomer pattern was calculated from the guessed set of fluxes. Without reduction, an unwieldy matrix with elements equal to the square of all of isotopomers in the cell would have to be inverted. However, there is another piece of information that can render this problem tenable: only a single source of isotope (1-<sup>13</sup>C glucose) was supplied to the cells. The amount of isotope in any isotopomer is therefore dependent only on the fluxes (pathways) that supply it with isotope. This is the basis for a tracing algorithm that generates an isotopomer matrix with only as many elements as the square of all isotopomers observed. This is more than two orders of magnitude smaller than the "brute force" approach and proportionally that much faster to solve.

*factor.* This factor scales from 0, irreversible, to 1, rapidly reversible, and can be incorporated seamlessly into the isotopomer matrix.

All of these advances in methodology enabled the analysis of the isotopomer data and an expansion of the metabolic model.

## B. Results and Discussion

### 1. TAM effects in MCF7 microcarrier cultures

MCF7 cells were subjected to 1  $\mu\text{M}$  TAM. The cell number on day 5 for TAM-treated flask was approximately 30% of the vehicle control flask. The growth curves are shown in Figure 4. Profiles of glucose, lactate, and glutamine concentrations as a function of time were determined and are shown in Figure 5. These profiles were then fit to a standard quadratic equation. The derivative of the fit was used to calculate uptake and production rates of glucose, lactate, and glutamine respectively. The results are shown in Table 2. Cell cycle phase was determined on day 5 and is shown in Figure 6. Cell morphology was documented using phase-contrast light microscopy and is shown in Figure 7.

	Glucose	Glutamine	Lactate
Control	4.2 $\pm$ 0.8	3.9 $\pm$ 0.7	1.4 $\pm$ 0.3
1 $\mu\text{M}$ TAM	0.0 $\pm$ 0.1	2.5 $\pm$ 0.1	4.8 $\pm$ 0.1

**Table 2. Uptake rates (mmol/day/ $10^9$  cells) for MCF7 microcarrier cultures, day 5.**

The above experiment indicated that certain metabolic effects of TAM can be quantified using microcarrier cultures. Glucose uptake on a per cell basis were significantly lower for TAM-treated cultures than for control cultures of MCF7 cells. Interestingly, lactate was consumed after several days in culture. This consumption was higher for TAM-treated cells. Lactate consumption did not occur in T47D cultures, for which data were presented in the last report. T47D cells showed less sensitivity to TAM and higher glycolytic capacity than MCF7 cells. This microcarrier data will be used for comparison to flux results obtained from cell extract experiments. Cell cycle analysis was used to investigate the nature of TAM action. The results indicate that TAM was acting as a cytostatic agent, causing cell cycle arrest in G0/G1.

### 2. Intracellular fluxes of estrogen-rescued MCF7 cells

The time response of glucose and lactate following estrogen-rescue, as described in the methods, is shown in Figure 8. The specific uptake of glucose and production of lactate both increased in the presence of estrogen. The NMR spectrum of the extract is shown in Figure 9. The areas of the labeled peaks were integrated and inputted into the algorithm to calculate the fluxes shown in figure 10.

There were a few fluxes that were significantly affected by estrogen. There was a six-fold increase in the pentose phosphate pathway (PPP) flux. This supports the hypothesis that estradiol stimulates the PPP in order to produce more NADPH, which is essential for biosynthesis. Pyruvate carboxylase and glutaminolysis both increased. These anaplerotic pathways supply the mitochondria with TCA cycle intermediates. These intermediates are the building blocks for many biosynthetic pathways. Again this supports the hypothesis that estrogen stimulates the biosynthetic pathways. The

preference for one of the two orientations of carbon scrambling in the TCA cycle supports the hypothesis that all of the TCA cycle enzymes are grouped into a complex that passes metabolites without releasing them freely into the bulk.

### 3. Preliminary Inhibitor Results

Six flasks were grown in different concentrations of cerulenin to determine which concentration would most effectively attenuate fatty acid synthase activity without causing cell death. The results are shown in Figure 11. A final working concentration of 26.9  $\mu\text{M}$  was chosen.

## C. Recommendations

The Statement of Work in the original proposal is included below. Recommendations in relation to the Statement of Work are given in Italics.

**Task 1:** Months 1-2: Serially wean MCF7 ER+, MCF7 ER-, and T47D ER+ cells to 2% serum. *Concerns were raised about the use of low levels of serum. MCF7 and T47D cell lines are being maintained in 5% serum.*

**Task 2:** Months 2-5: Implement more precise analytical control and monitoring capabilities of existing hollow fiber bioreactor (HFBR) support apparatus. *A more robust temperature control algorithm implementing cascade control has been created. This controller is capable of maintaining the desired set point ( $37^\circ\text{C}$ ) plus or minus  $0.1^\circ\text{C}$ . However, this system will not be used since data obtained from batch extraction experiments afford significantly higher accuracy. In an extraction experiment it is possible to obtain a 100-fold increase in NMR sensitivity. An experiment takes one week as opposed to three months and can test more than 6 conditions as opposed to 1 in an HFBR.*

**Task 3:** Months 5-6: Treat HFBR with attachment factors and test cell growth. *T47D cells were grown in an HFBR for 3 months at which point the cells were removed by trypsinization. Both NMR and culturing techniques indicated that there was little viability in the 5g cell pellet. A modified HFBR would be needed to attain a higher viable cell density. To overcome the difficulties with the HFBR apparatus, roller bottles are used to obtain the necessary inputs for flux analysis.*

**Task 4:** Months 7-8: Perform growth studies to determine cerulenin concentration to be used in HFBR experiments. *This task has been completed.*

**Task 5:** Month 9: Inject treated HFBR with ER+ MCF7 cells and allow them to grow to high density. *See Task 3.*

**Task 6:** Months 10-14: Execute serial step changes in medium composition, such as TAM concentration and  $^{13}\text{C}$ -labeled metabolites, while continually measuring internal and external metabolites. *Serial step changes were not performed, but equivalent information was obtained.*

**Task 7:** Month 15-16: Perform cell extract experiments to confirm spectral assignment of metabolites. *As was described in Materials and Methods, the extraction technique proved to be more*

*beneficial than expected. The ability to detect isotopic distribution by <sup>13</sup>C-NMR measurements of extracts prompted us to use cell extract methodology for all subsequent experiments.*

**Task 8:** Months 17-18: Perform data analysis. Check for inconsistencies with existing metabolic model. *It was possible to perform this task with <sup>13</sup>C-NMR extract measurements. As described in the results section, many models have been tested and a simulation method has been developed to discern between models.*

**Task 9:** Month 19: Inject treated HFBR with ER+ T47D cells and allow to grow to high density. *See task 3.*

**Task 10:** Months 20-28: Repeat tasks 6-8 but for the T47D cell line.

**Task 11:** Month 28: Inject treated HFBR with ER- MCF7 cells and allow to grow to high density. *See task 3.*

**Task 12:** Months 29-36: Repeat tasks 6-8 but for the ER- cell line.

## **KEY RESEARCH ACCOMPLISHMENTS**

- Identified key operative metabolic pathways in ER+ MCF7 breast cancer cells
- Developed novel methodology employing NMR data, including isotopomers, from cell extracts and a metabolic model to calculate intracellular fluxes
- Used this methodology to characterize metabolic responses of MCF7 cells to estrogen and tamoxifen

## **REPORTABLE OUTCOMES**

Forbes, N.S., Blanch, H.W. and Clark, D.S. "Metabolic Flux Analysis to Characterize the Response of Human Breast Cancer Cells to Hormones," poster presented at the Metabolic Engineering II Meeting, Elman, Germany, October 25 1998.

Forbes, N.S., Blanch, H.W. and Clark, D.S. "Analysis of Metabolic Fluxes in Mammalian Cells". In: Bioreaction Engineering: Modelling and Control. Eds. Schugerl, K., Bellgardt, K. Springer-Verlag, Berlin, Germany, in press.

Wicklund, K.A., Blanch, H.W. and Clark, D.S. "Characterization of Human Breast Cancer Cells in Microcarrier Culture: Effects of Glucose and Oxygen," poster presented at the Whitaker Foundation Annual Meeting, La Jolla, CA, August 18, 1999.

Wicklund, K. A., Blanch, H.W. and Clark, D.S. "Characerization of Human Breast Cancer Cells in Microcarrier Culture," presented at the American Chemical Society National Meeting, Anaheim, CA, March 25, 1999.

Wicklund, K.A., Blanch, H.W. and Clark, D.S. "Effects of Glucose and Oxygen on MCF7 Metabolism and Response to Tamoxifen." Manuscript in preparation.

## **CONCLUSIONS**

In summary, we have developed advanced methodology that has allowed us to investigate the metabolic consequences of estrogen and tamoxifen treatment. We have identified for the first time isotopomers following 1-<sup>13</sup>C glucose treatment, which was enabled by advances in the proposed technique. We have also developed an algorithm to analyze isotopomer data that is fast, general, and increases the accuracy and extent of flux calculations. These improvements in methodology have allowed us to quantify more completely internal metabolic fluxes in ER+ human breast cancer cells following estrogen rescue. Results from this analysis have confirmed our hypothesis about the action of estrogen. Specifically, increases in the pentose phosphate pathway, glutaminolysis, and flux through pyruvate carboxylase were observed following estrogen stimulation. Finally, we have completed preliminary investigations using the fatty acid synthase inhibitor, cerulenin.

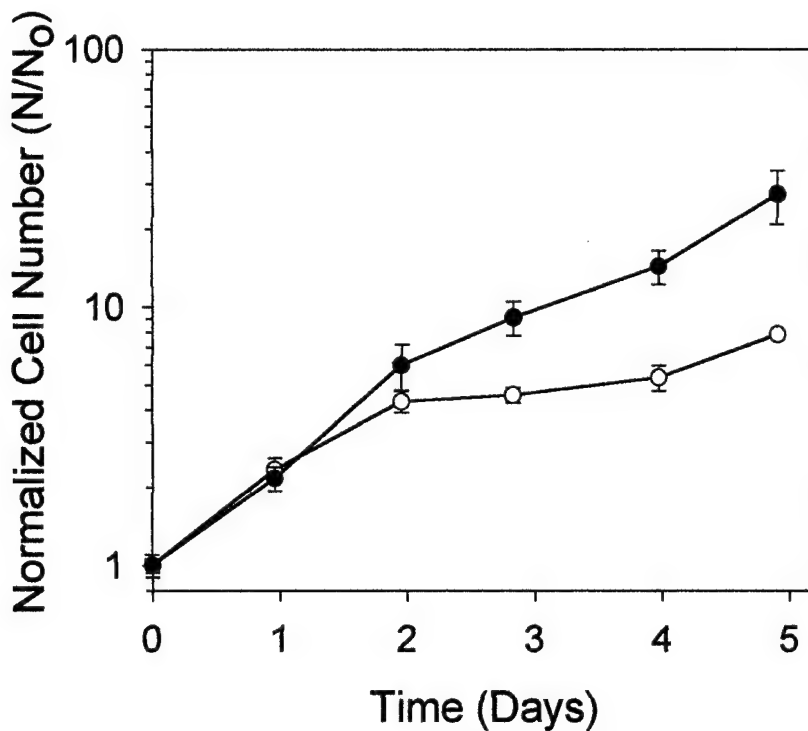


**Figure 4:** Growth curve for MCF7 microcarrier cultures. Cultures were fed 1mM TAM or vehicle control on day 0. Error bars represent standard deviation of triplicate measurements.

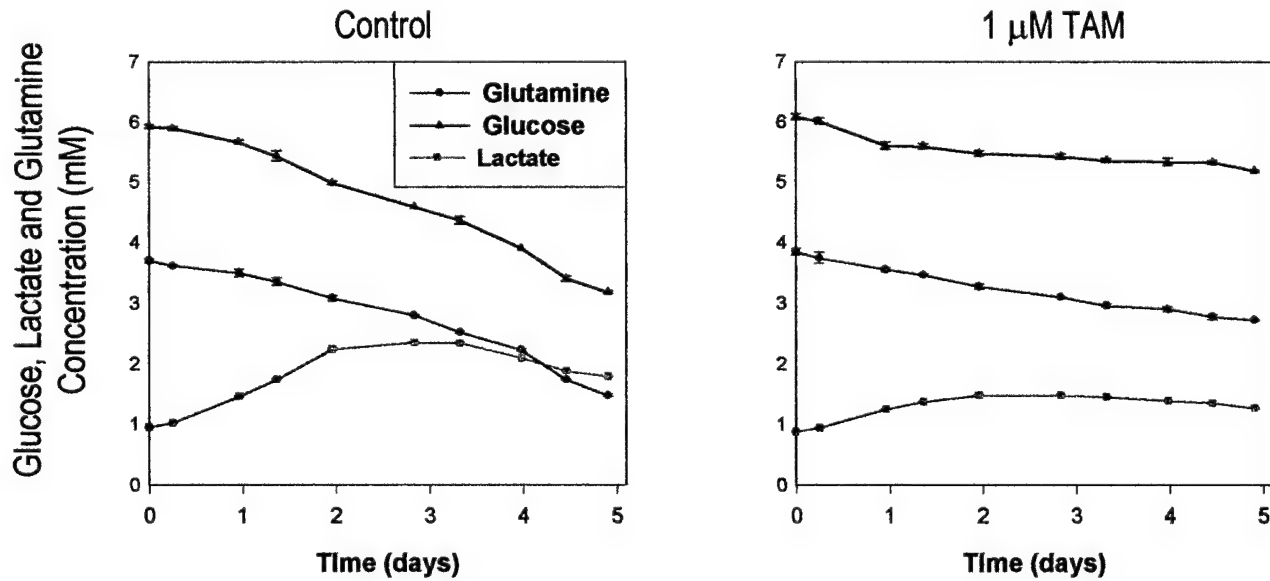


**Figure 5:** Glucose, lactate, and glutamine concentrations as a function of time for MCF7 microcarrier cultures.

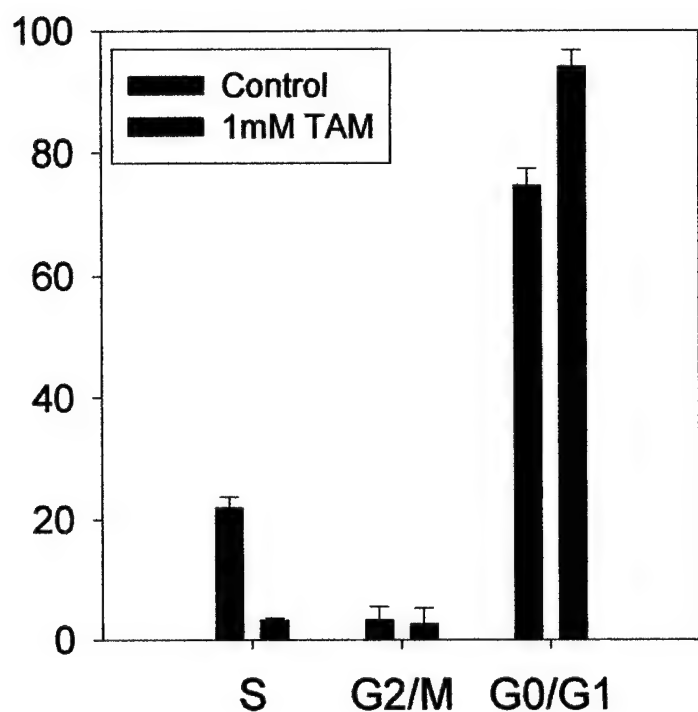


Figure 6: Cell cycle analysis of MCF7 microcarrier cultures on day 5

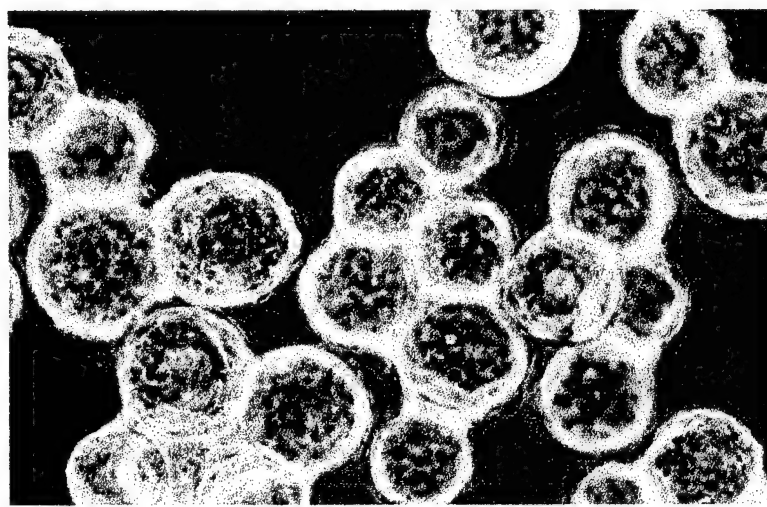


Figure 7: Phase-contrast light microscopy image of MCF7 microcarrier control cultures on day 5.

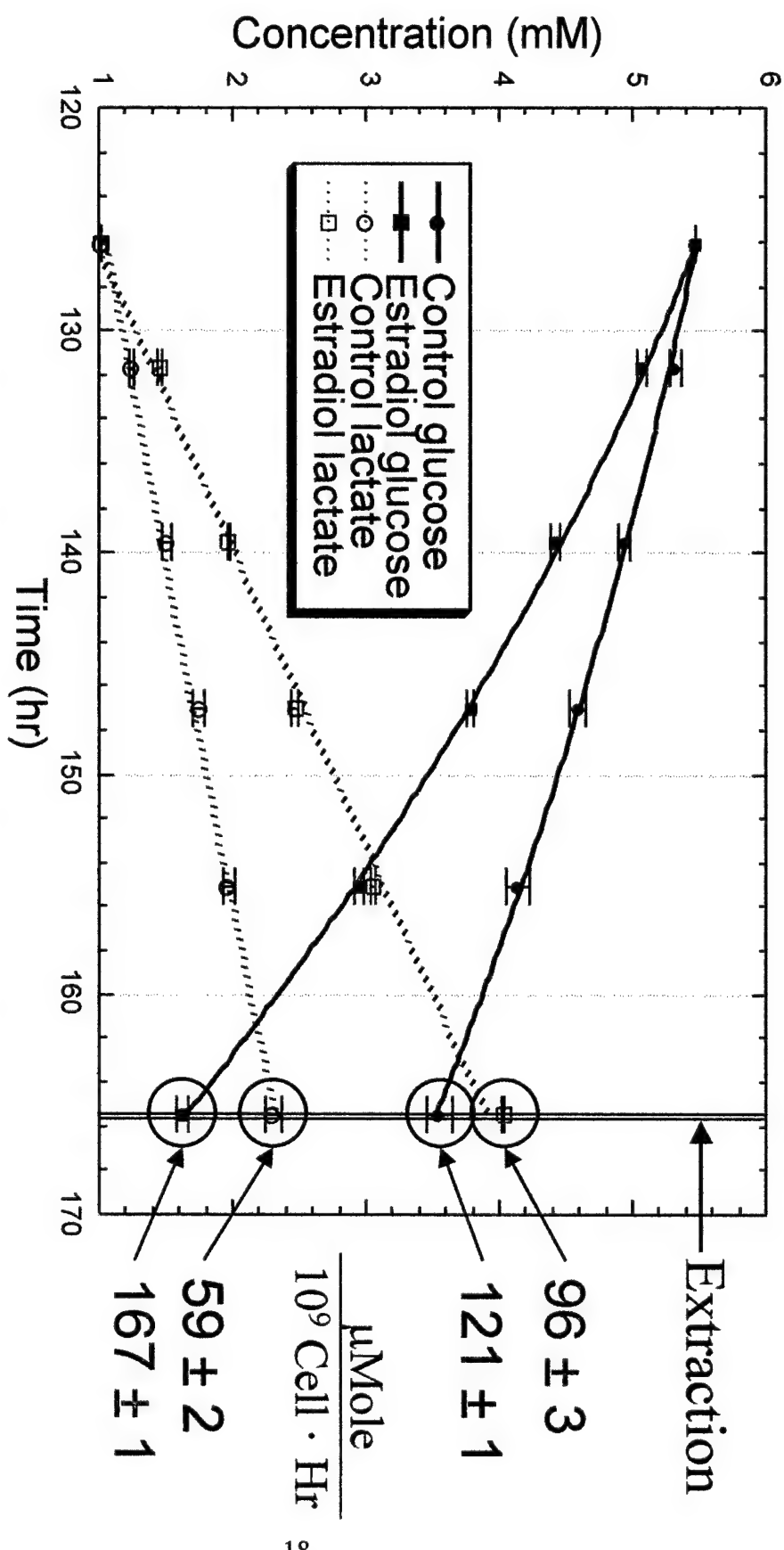


Figure 8. Glucose and lactate response following estradiol treatment of MCF7 cells.  
External fluxes calculated by normalizing the first derivative of the concentration vs. time profile by the cell number.

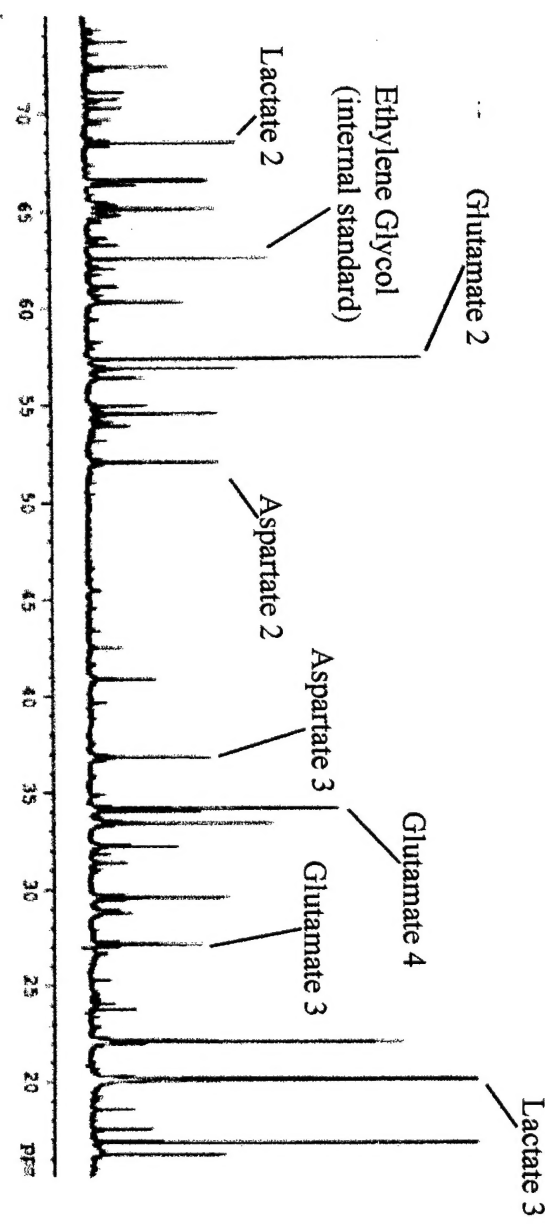


Figure 9. NMR spectrum of the cytosolic extract from estradiol stimulated MCF7 cells. The relevant peaks for metabolic flux analysis are labeled

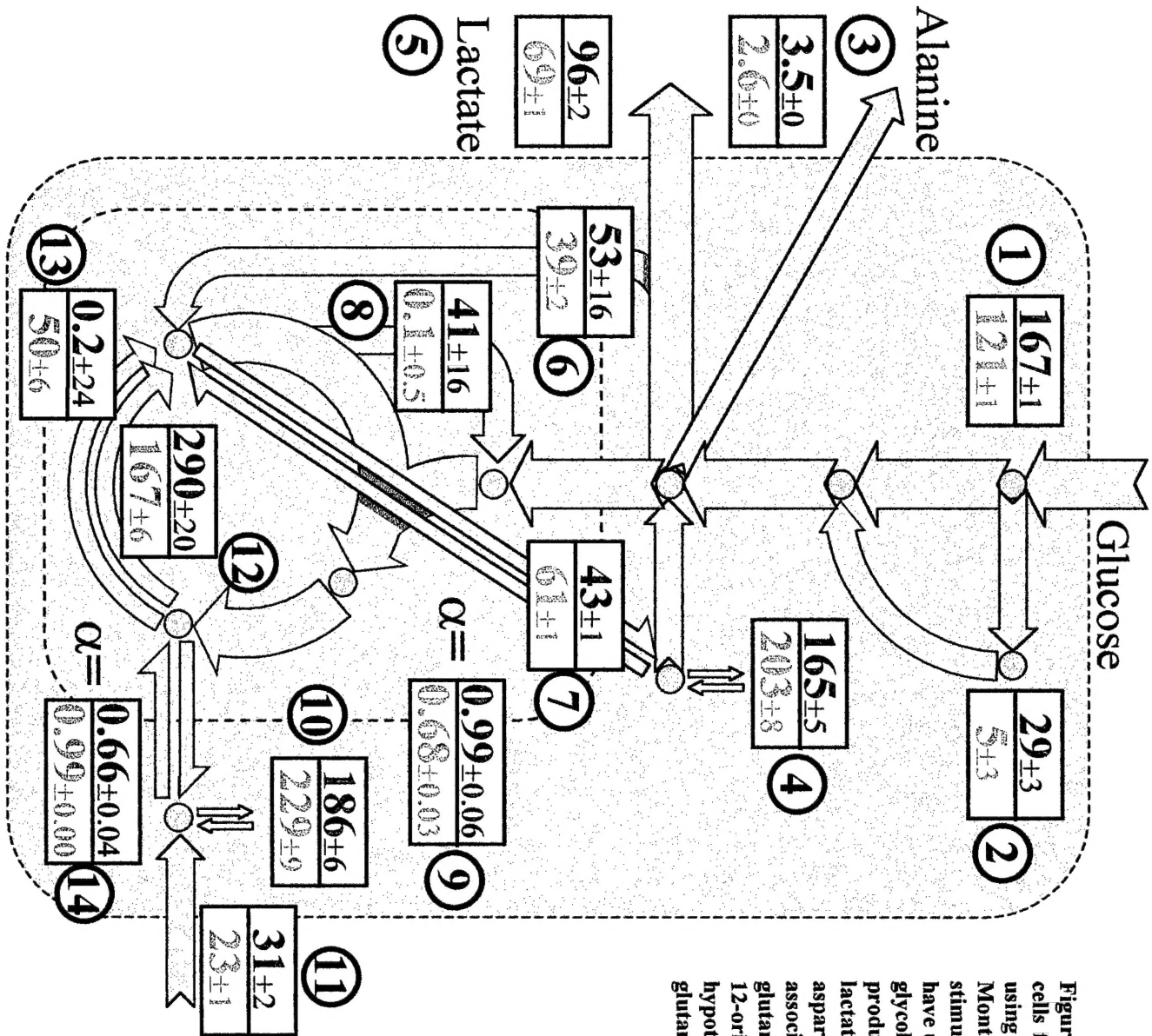
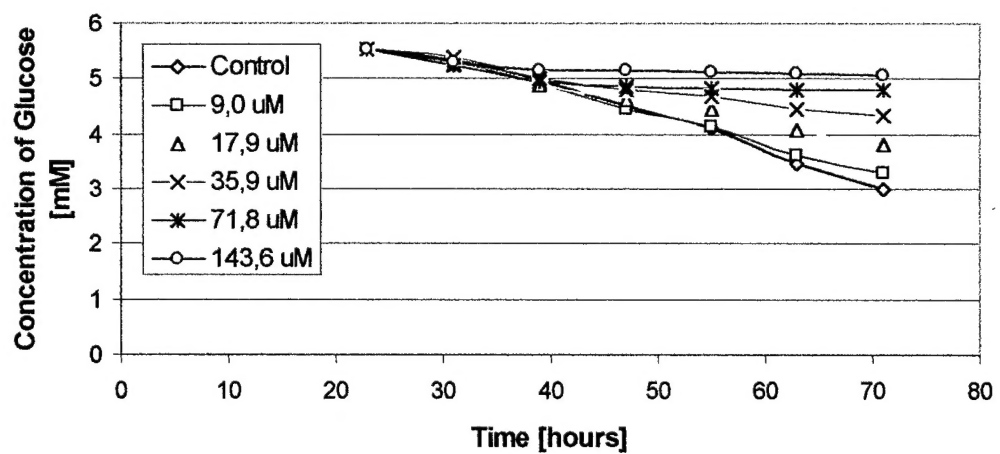


Figure 10. Fluxes in the internal pathways of MCF7 cells following estrogen rescue. Fluxes were calculated using simulated annealing and errors were calculated by Monte Carlo simulation. The red top fluxes are estradiol stimulated and the green bottom are control. All fluxes have units of  $\mu\text{Mole} / (10^9 \text{ cell} \cdot \text{hr})$ . The pathways are: 1-glycolysis, 2-the pentose phosphate pathway, 3-alanine production, 4-aspartate incorporation into protein, 5-lactate production, 6-pyruvate carboxylase, 7-malate-aspartate shuttle, 8-intramitochondrial malic enzyme, 9-association factor for malate aspartate shuttle, 10-glutamate incorporation into protein, 11-glutaminoylation, 12-orientation one of citric acid cycle (tests channelling hypothesis), 13-orientation two, 14-association factor for glutamate exchanging into mitochondria.



**Figure 11:** Effect of different concentrations of cerulenin on the glucose uptake rate of MCF7 cells.

## **REFERENCES**

1. Paik S, Harmann D, Dickson R, Lippman M. Antiestrogen resistance in ER positive breast cancer cells. *Breast Cancer Res Treatment*. 1994;31:2-3:301-7.
2. Frehney, R. *Culture of animal cells: a manual of basic technique*. New York: Alan R. Liss, Inc.
3. Kueng W, Silber E, Eppenberger U. Quantification of cells cultured on 96-well plates. *Analytical Biochemistry*. 1989;182:16-19.
4. Van Wezel A. Microcarrier cultures of animal cells. In: Kruse PF, Patterson MK, eds. *Tissue Culture: Methods and Applications*. New York: Academic Press; 1973, pp. 372-377.
5. Degani H, DeJordy J, Salomon Y. Stimulation of cAMP and phosphomonoester production by melanotropin in melanoma cells:  $^{31}\text{P}$  NMR studies. *Proceedings of the National Academy of Science*. 1990;88:1506-1510.
6. Blanch B, Clark D. *Biochemical Engineering*. New York: Marcel Dekker, Inc.; 1996.
7. Zupke C, Stephanopoulos G. Intracellular flux analysis in hybridomas using mass balances and in vitro  $^{13}\text{C}$  NMR. *Biotechnology and Bioengineering*. 1995;45:292-303.
8. Chandler J, Hill D, Spivey H. A program for efficient integration of rate equations and least-squares fitting of chemical reaction data. *Computers and Biomedical Research*. 1972;5:515-534.